Supporting Information

Tuning the Optical Properties of the Metal-organic Framework UiO-66 via Ligand Functionalization

Marvin Treger[1,2], Adrian Hannebauer[1], Andreas Schaate[1], Jan L. Budde[1], Peter Behrens[1,2] and Andreas M. Schneider[1,2]

[1]Institute of Inorganic Chemistry, Leibniz University Hannover, Callinstr. 9, 30167 Hannover, Germany
[2]Cluster of Excellence PhoenixD (Photonics, Optics, and Engineering – Innovation Across Disciplines), Hannover, Germany

Table of Contents

Section 1 Experimental Details

Chemicals

Zirconium (IV) chloride (>99.5%, $ZrCl_4$, Sigma Aldrich), (>98%, $ZrOCl_2 \cdot 8\ H_2O$, Sigma Aldrich), *N,N*-dimethylformamide (99.8%, DMF, Sigma Aldrich), acetic acid (>99.7%, CH_3COOH, Sigma Aldrich), formic acid (>98%, HCOOH, Merck), terephthalic acid (99%, $C_8H_6O_4$ (H_2BDC), Honeywell), 2-nitroterephthalic acid (>99%, $C_8H_5O_6N$ ($H_2BDC\text{-}NO_2$), Sigma Aldrich), 2-aminoterephthalic acid (99%, $C_5H_7O_4N$ ($H_2BDC\text{-}NH_2$), Sigma Aldrich) were used without purification.

Synthesis of $H_2BDC\text{-}(NH_2,NO_2)$

This linker was synthesized according to published procedures.[1,2]

25 g (119.5 mmol) dimethyl 2-aminoterephthalate were dispersed in 95 mL of dry toluene. To this suspension 16.7 mL (176.7 mmol) acetic anhydride was added and the mixture was heated to 80 °C. The solid was completely dissolved after 15 minutes. The heating was continued for a total of 2 h. During this time copious amounts of a white solid precipitated. After cooling to room temperature, the solid was filtered and washed with cold toluene. It was recrystallized from 250 mL of toluene and dried over night at 80 °C in an oven and an additional hour at 120 °C to give 20.8 g (69%) of dimethyl 2-acetamidoterephthalate.

20.8 g of dimethyl 2-acetamidoterephthalate were dispersed in 35 mL concentrated sulfuric acid and cooled with an ice bath. To the stirred suspension a cooled nitrating acid solution (40 mL concentrated sulfuric acid and 50 mL fuming nitric acid) was added dropwise within 20 minutes so that the temperature was between 10 and 20 °C. The mixture was stirred for an additional hour at 0 °C. Most of the solid dissolved during the addition of the nitrating acid, the small amount of residual solid was separated from the solution with a spatula and discarded. The solution was poured onto 460 g of ice after upon which a yellow solid precipitated. The mixture was stored at room temperature overnight and filtered on the next day. Then it was washed with diluted $NaHCO_3$ solution and finally with water. The crude solid was recrystallized from 320 mL methanol and dried at room temperature to give 12.3 g (50%) dimethyl 2-acetamido-5-nitroterephthalate.

12.3 g dimethyl 2-acetamido-5-nitroterephthalate were dissolved in 240 mL THF. To this solution 240 mL of KOH solution (4%) were dropped. The colour of the solution changed from yellow to deeply red. It was heated at reflux for 24 h. The THF of the solution was then removed using a rotary evaporator. 200 mL of HCl solution (1M) were added to the solution and a yellow precipitate formed. The suspension was stored in a refrigerator overnight and filtered and washed with water the next day. The product was dried at 120 °C in an oven to give 8.3 g (88%) of the linker.

Synthesis of MOFs

<u>UiO-66</u>

According to Shearer *et al*.,[3] nearly defect-free UiO-66 was synthesized by sequentially adding 0.777 g $ZrCl_4$ (1 eq), 0.552 mL 37% HCl (2 eq) and 1.104 g H_2BDC (2 eq) to 20 mL DMF (77.5 eq) to a beaker. After stirring this solution for 30 minutes a clear solution was obtained which was transferred to a Teflon liner and sealed in a stainless-steel autoclave, which was heated at 220 °C for 20 h. The resulting white powder was separated via centrifugation, washed with DMF and acetone and dried under vacuum overnight. Afterwards the powder was purified using a Soxhlet-extraction with acetone for 24 h and activated at 150 °C for 20 h.

UiO-66-NO_2

UiO-66-NO_2 was synthesized in a 100 mL Pyrex glass vessel by sequentially adding 0.3010 g $ZrCl_4$ (1 eq), 2.436 mL formic acid (50 eq) and 0.2727 g $H_2BDC{-}NO_2$ in 25 mL DMF (250 eq). The glass vessel was sealed and heated at 120 °C for 24 h. The resulting powder was separated via centrifugation, washed with DMF and acetone and dried under vacuum overnight.

UiO-66-NH_2

UiO-66-NH_2 was synthesized in a 100 mL Pyrex glass vessel by sequentially adding 0.6468 g $ZrCl_4$ (1 eq), 3.968 mL acetic acid (25 eq) and 0.5028 g $H_2BDC{-}NH_2$ in 10 mL deionized water (200 eq). The glass vessel was sealed and heated at 120 °C for 24 h. The resulting powder was separated via centrifugation, washed with deionized water and acetone and dried under vacuum overnight.

UiO-66-(NH_2,NO_2)

UiO-66-(NH_2,NO_2) was synthesized in a 100 mL Pyrex glass vessel by sequentially adding 0.2972 g $ZrOCl_2 \cdot 8\ H_2O$ (1 eq), 5.274 mL acetic acid (100 eq) and 0.2085 g H_2BDC-(NH_2,NO_2) (1 eq) in 7.14 mL DMF (100 eq). The glass vessel was sealed and heated at 150 °C for 12 h. The resulting powder was separated via centrifugation, washed with DMF and acetone and dried under vacuum overnight.

Characterization of UiO-66-(NH_2,NO_2)

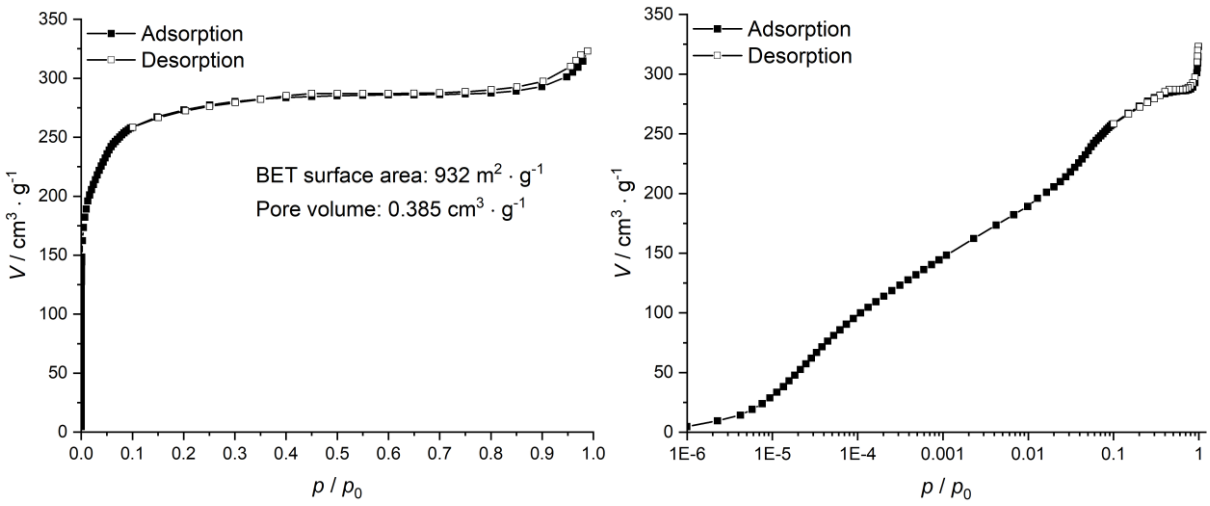

Figure S1. Ar sorption @ 87 K of UiO-66-(NH_2,NO_2).

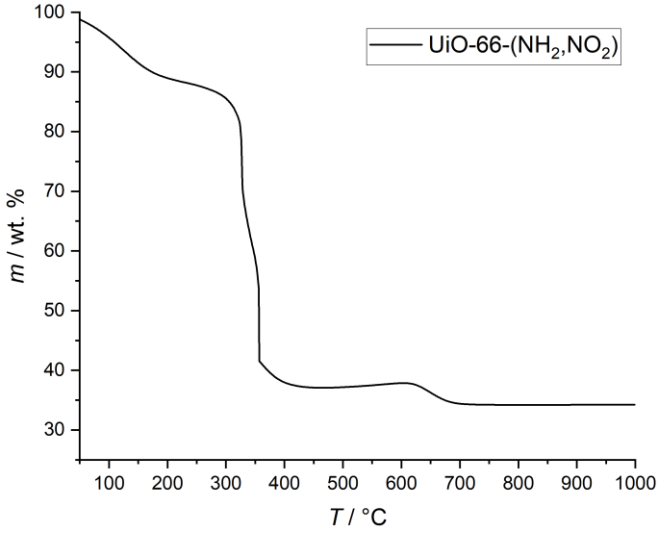

Figure S2. Thermogravimetric measurement of UiO-66-(NH_2,NO_2).

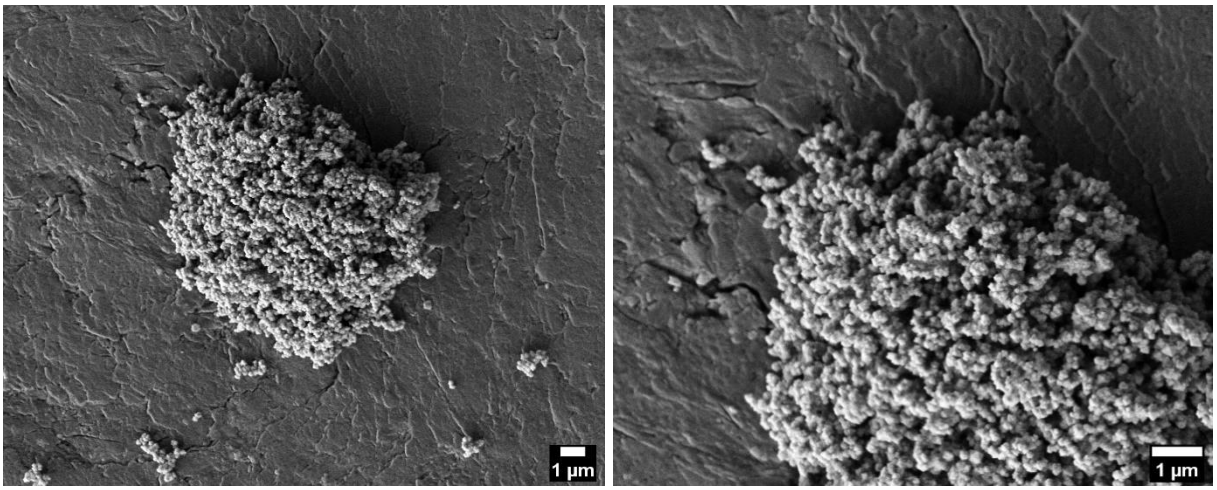

Figure S3. SEM images of UiO-66-(NH_2,NO_2).

NMR Spectra

The successful non-destructive incorporation of the linkers into the framework and the absence of guest molecules after washing and drying the powders was monitored with ^{1}H-NMR-spectroscopy on digested samples. For this instance, 15 mg of MOF were digested in 1 M NH_4CO_3 solution in D_2O for 2 h.

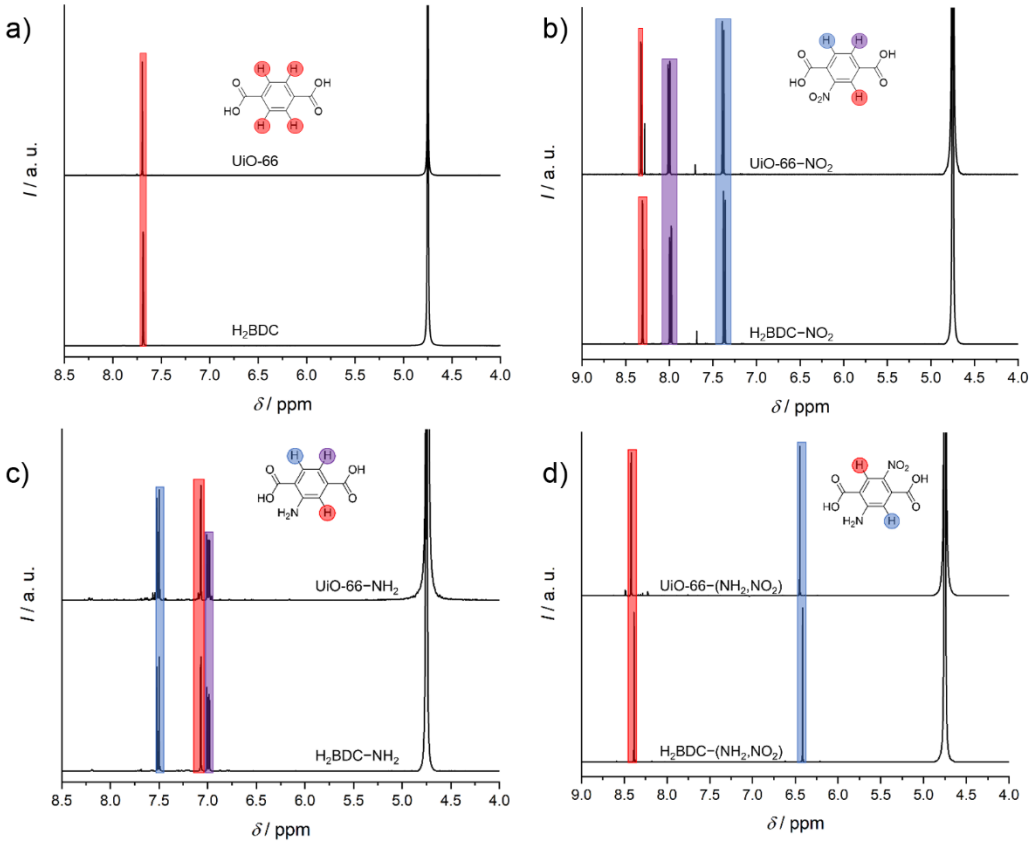

Figure S4. ^{1}H NMR spectra of digested MOFs compared to the linker. a) UiO-66. b) UiO-66−NO_2. c) UiO-66−NH_2. d) UiO-66-(NH_2,NO_2).

UV-Vis Spectra

To validate the electronic structure calculations, UV-Vis DRS was performed.

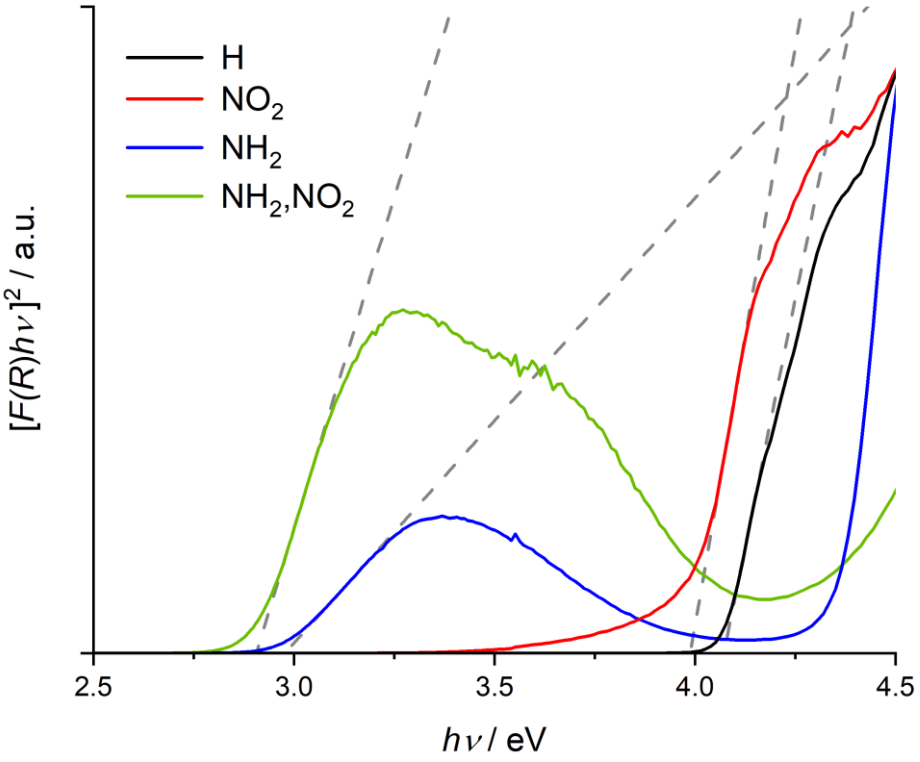

Figure S5. Tauc plot of recorded UV-Vis spectra.

Section 2 Plane wave basis set convergence

The kinetic plane wave energy cutoff convergence was tested with respect to the lattice parameter *a* of the primitive cells and the threshold was set to a change of 0.01 Å. The sampling of the Brillouin zone was tested with respect to the total energy and the lattice parameter *a* of the primitive cells.

UiO-66

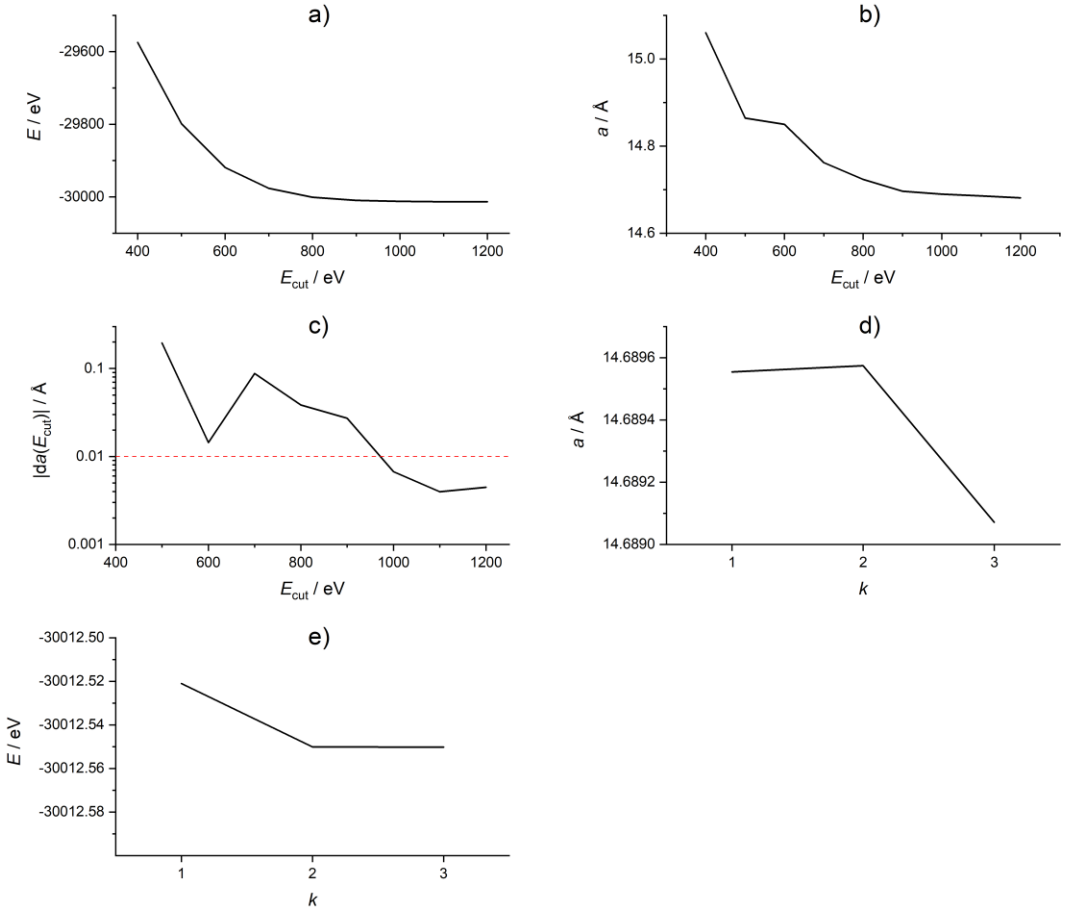

Figure S6. UiO-66: Convergence of a) total energy, b) lattice parameter *a*, c) lattice parameter *a* (derivation), d) *k* points (energy) and e) *k* points (lattice).

UiO-66-NO_2

The basis set convergence of the UiO-66 derivates (*P*1 space group) was tested on the basis of the averaged lattice parameter (standard error is shown).

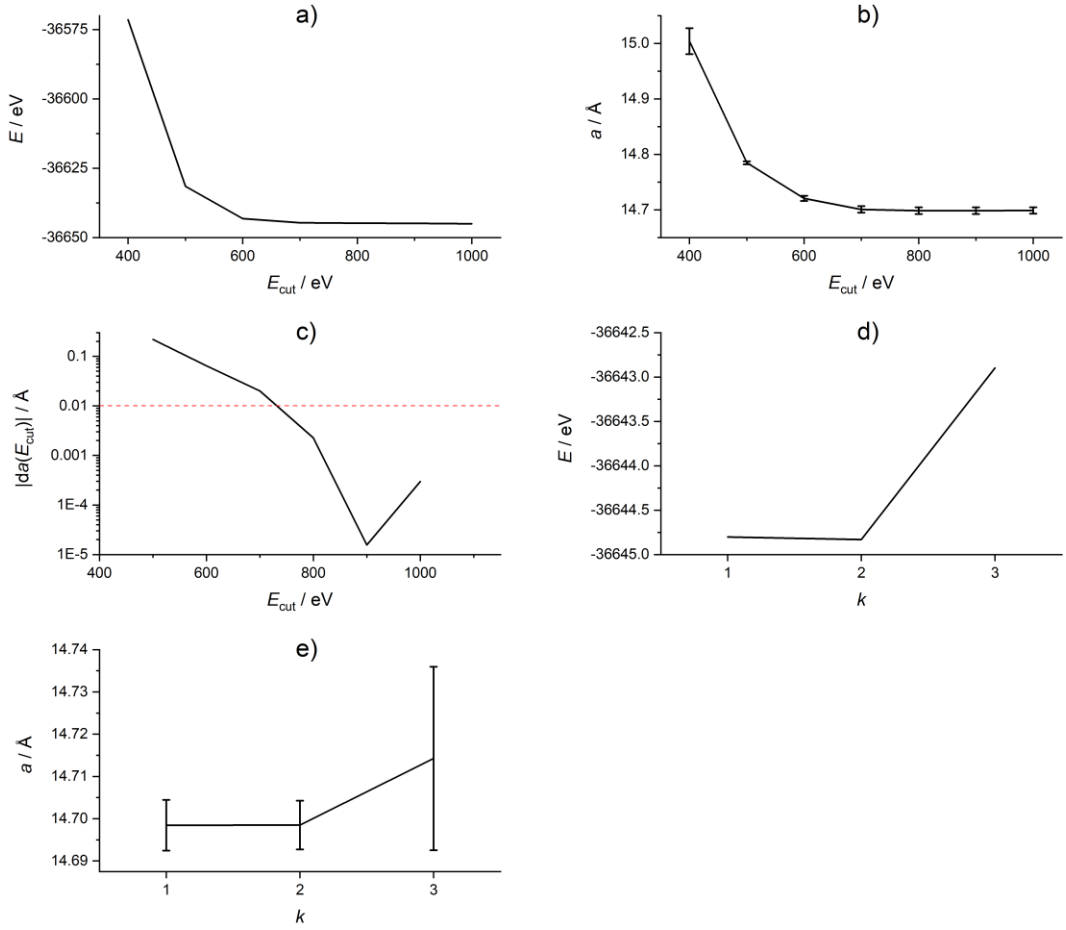

Figure S7. UiO-66-NO_2: Convergence of a) total energy, b) lattice parameter *a*, c) lattice parameter *a* (derivation), d) *k* points (energy) and e) *k* points (lattice).

UiO-66-NH_2

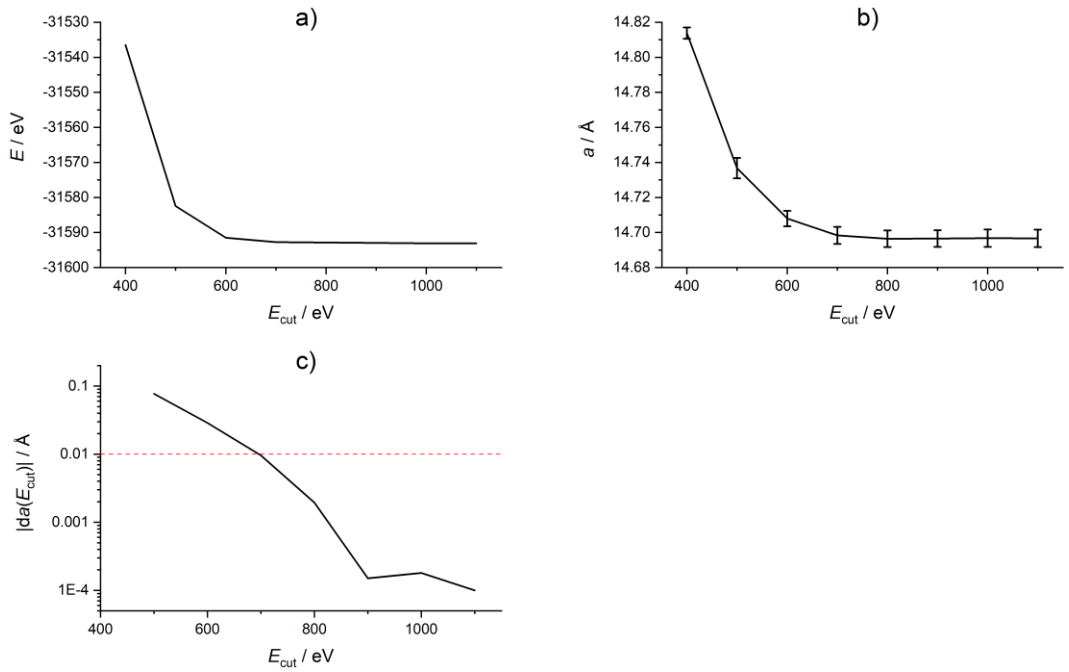

Figure S8. UiO-66-NH_2: Convergence of a) total energy, b) lattice parameter *a* and c) lattice parameter *a* (derivation).

UiO-66-(NH_2,NO_2)

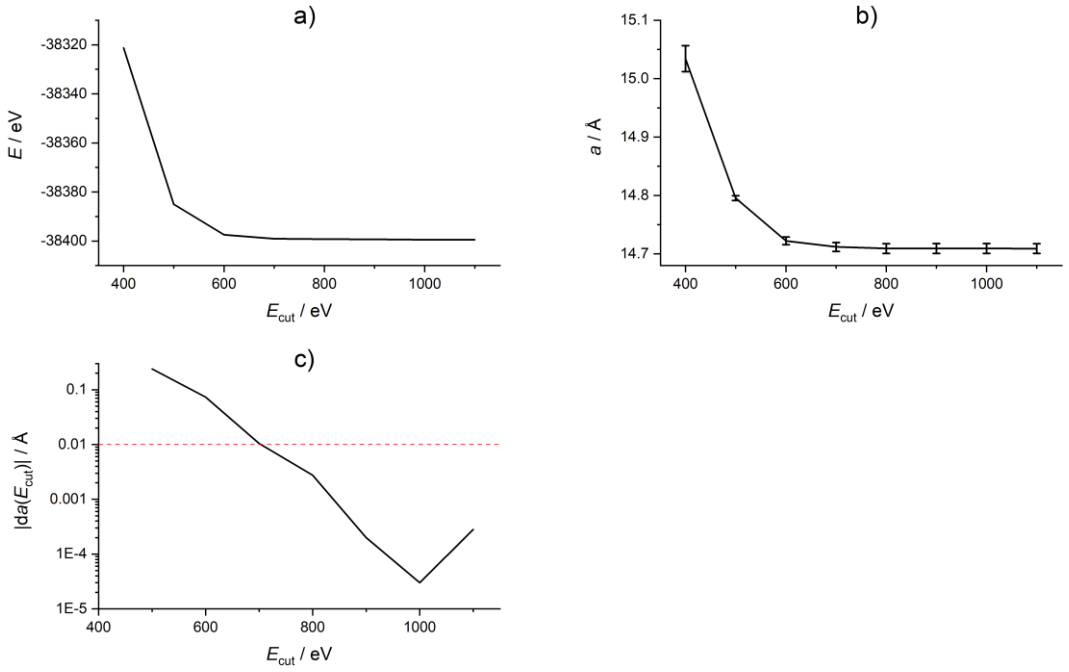

Figure S9. UiO-66-(NH_2,NO_2): Convergence of a) total energy, b) lattice parameter *a* and c) lattice parameter *a* (derivation).

UiO-66-(N(Me)$_2$,NO$_2$)

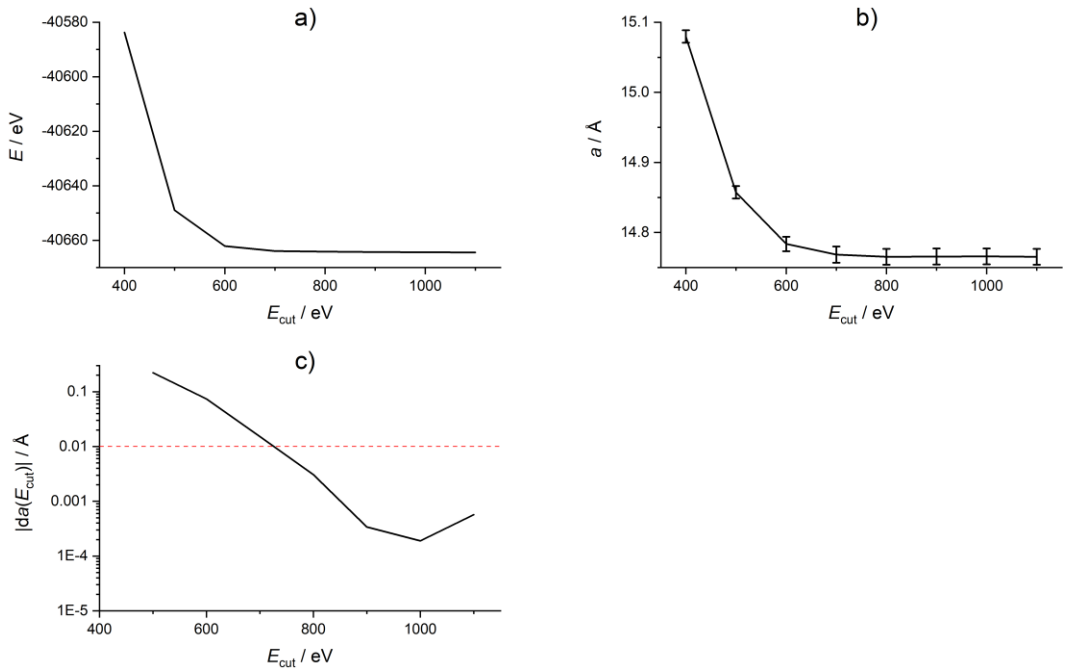

Figure S10. UiO-66-(N(Me)$_2$,NO$_2$): Convergence of a) total energy, b) lattice parameter *a* and c) lattice parameter *a* (derivation).

UiO-66-(NH$_2$,DCV)

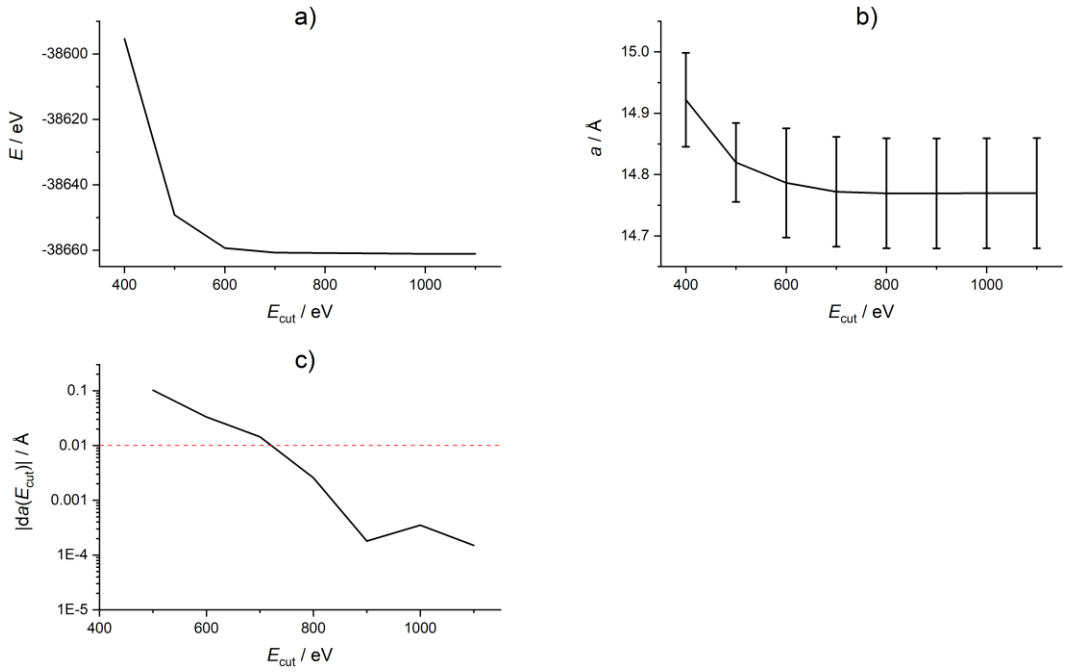

Figure S11. UiO-66-(NH$_2$,DCV): Convergence of a) total energy, b) lattice parameter *a* and c) lattice parameter *a* (derivation).

UiO-66-(N(Me)$_2$,DCV)

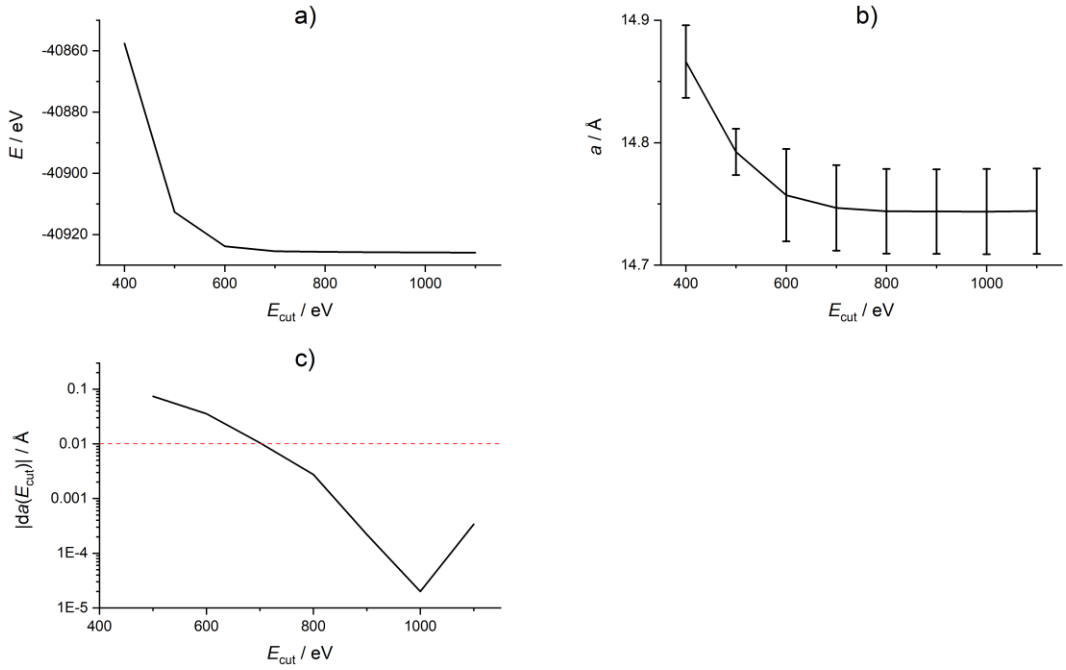

Figure S12. UiO-66-(N(Me)$_2$,DCV): Convergence of a) total energy, b) lattice parameter *a* and c) lattice parameter *a* (derivation).

Section 3 XC functional benchmark

In the case of the UiO-66 derivates (*P*1 space group) the XC functionals were examined on the basis of the averaged lattice parameter (standard error is shown).

UiO-66

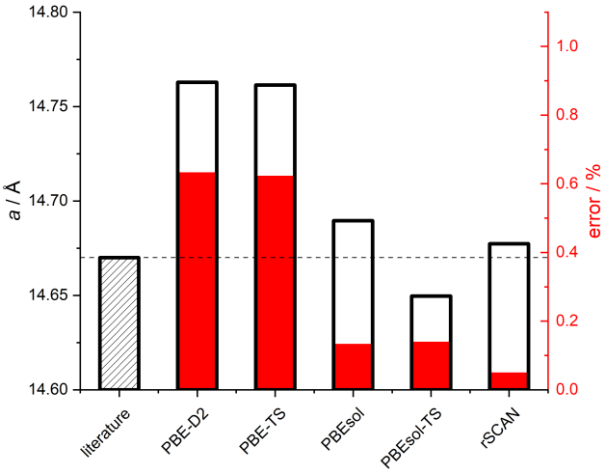

Figure S13. UiO-66: XC functional benchmark (absolute value black with relative error in red).

UiO-66-NO_2

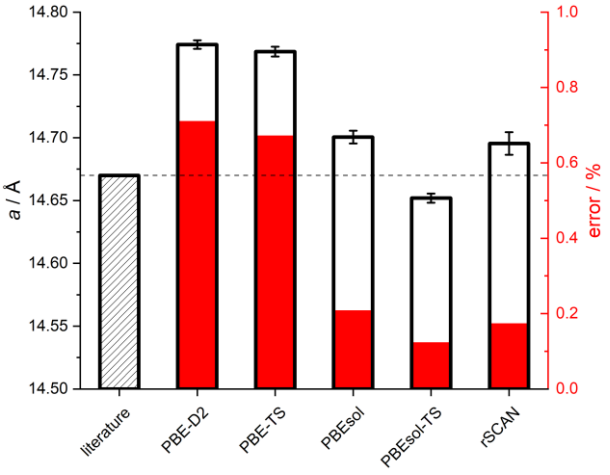

Figure S14. UiO-66-NO_2: XC functional benchmark (absolute value black with relative error in red).

UiO-66-NH_2

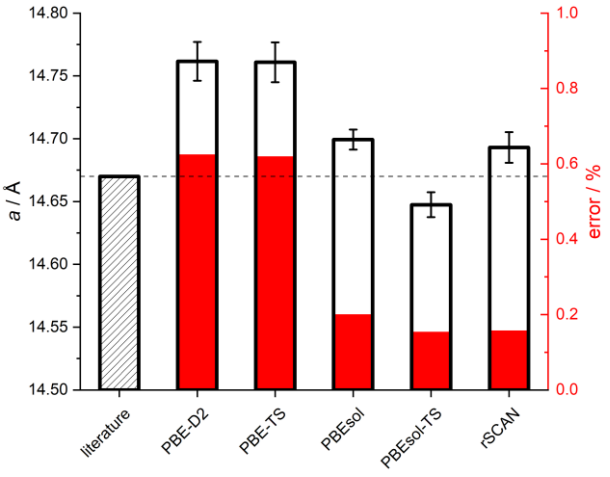

Figure S15. UiO-66-NH_2: XC functional benchmark (absolute value black with relative error in red).

UiO-66-(NH_2,NO_2)

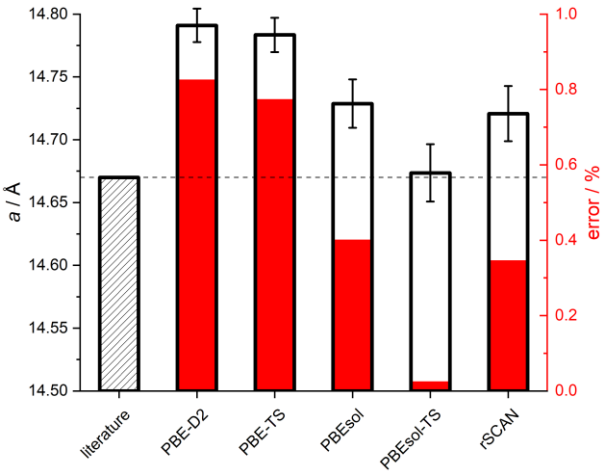

Figure S16. UiO-66-(NH_2,NO_2): XC functional benchmark (absolute value black with relative error in red).

UiO-66-(N(Me)$_2$,NO$_2$)

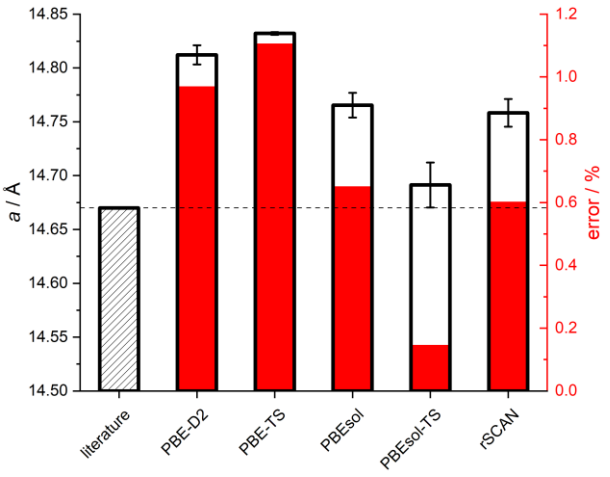

Figure S17. UiO-66-(N(Me)$_2$,NO$_2$): XC functional benchmark (absolute value black with relative error in red).

UiO-66-(NH$_2$,DCV)

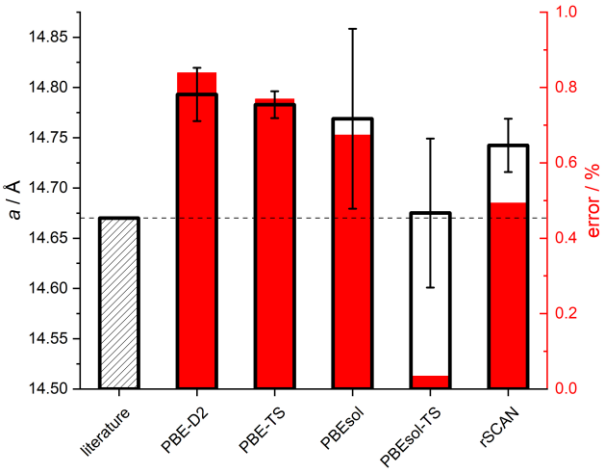

Figure S18. UiO-66-(NH$_2$,DCV): XC functional benchmark (absolute value black with relative error in red).

UiO-66-(N(Me)$_2$,DCV)

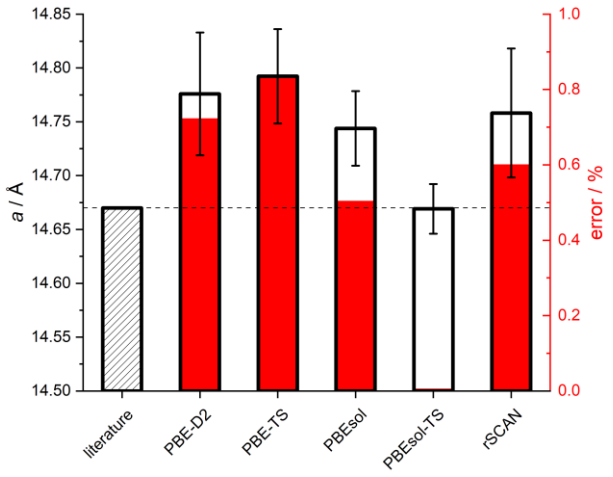

Figure S19. UiO-66-(N(Me)$_2$,DCV): XC functional benchmark (absolute value black with relative error in red).

Section 4 Band structures

Table S1. Comparison of calculated and experimental band gaps.

MOF	sim. / eV	exp. / eV
UiO-66	4.25	4.05
UiO-66-NO_2	3.92	3.06
UiO-66-NH_2	2.83	2.91
UiO-66-(NH_2,NO_2)	2.78	2.68
UiO-66-($N(Me)_2$,NO_2)	2.37	-
UiO-66-(NH_2,DCV)	2.31	-
UiO-66-($N(Me)_2$,DCV)	2.31	-

UiO-66

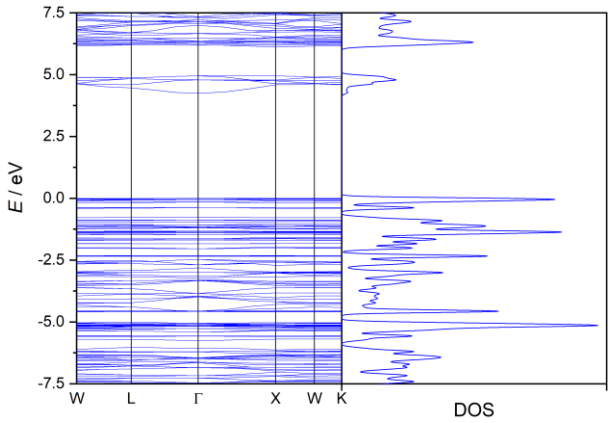

Figure S20. UiO-66 band structure with DOS.

UiO-66-NO_2

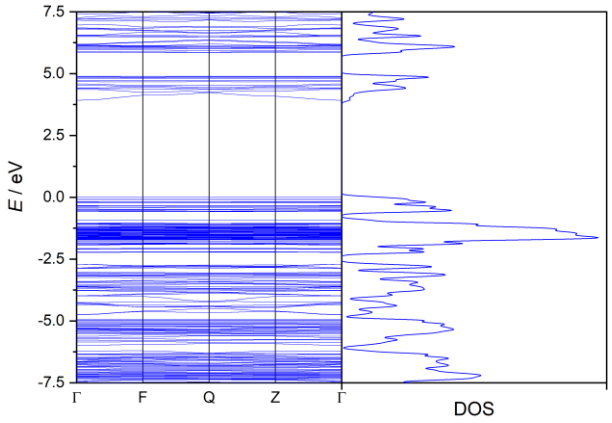

Figure S21. UiO-66-NO_2 band structure with DOS.

UiO-66-NH_2

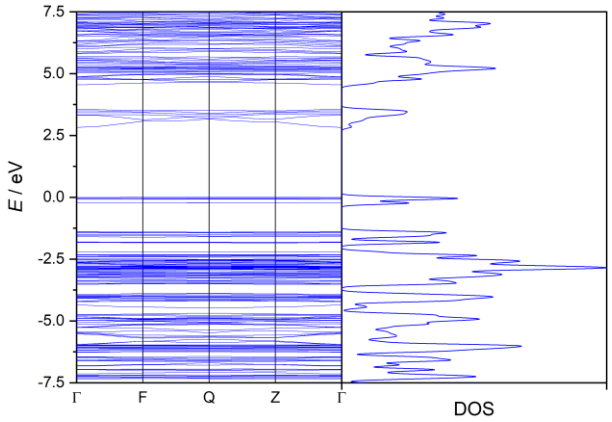

Figure S22. UiO-66-NH_2 band structure with DOS.

UiO-66-(NH_2,NO_2)

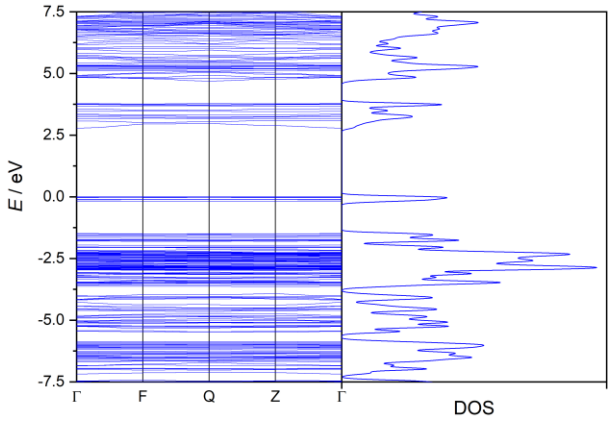

Figure S23. UiO-66-(NH_2,NO_2) band structure with DOS.

UiO-66-(N(Me)$_2$,NO$_2$)

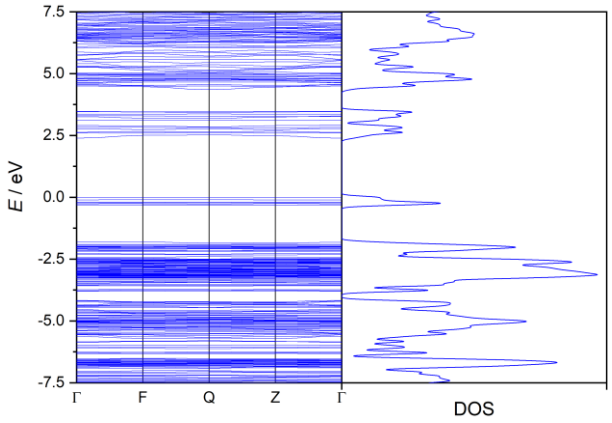

Figure S24. UiO-66-(N(Me)$_2$,NO$_2$) band structure with DOS.

UiO-66-(NH$_2$,DCV)

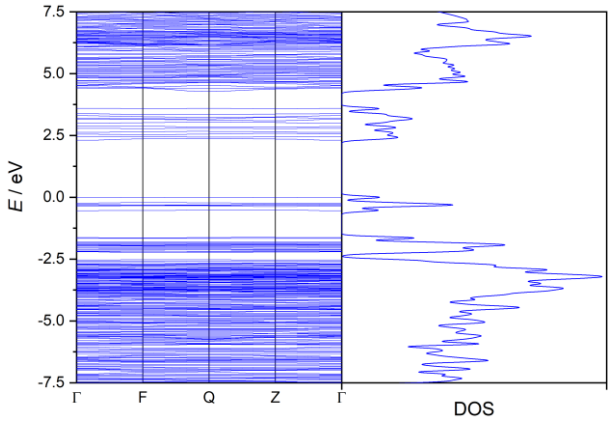

Figure S25. UiO-66-(NH$_2$,DCV) band structure with DOS.

UiO-66-(N(Me)$_2$,DCV)

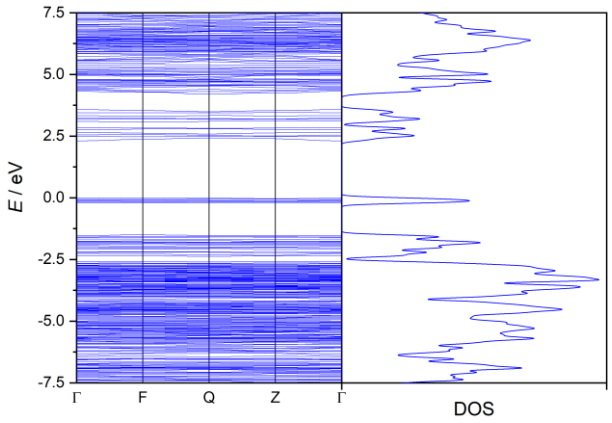

Figure S26. UiO-66-(N(Me)$_2$,DCV) band structure with DOS.

Section 5 Refractive Index

Table S2. Comparison of calculated refractive indices at 589 nm.

MOF	n_{589}
UiO-66	1.373
UiO-66-NO_2	1.408
UiO-66-NH_2	1.419
UiO-66-(NH_2,NO_2)	1.503
UiO-66-(N(Me)$_2$,NO_2)	1.600
UiO-66-(NH_2,DCV)	1.736
UiO-66-(N(Me)$_2$,DCV)	1.776

Section 6 Calculation of the refractive index with the PBE XC functional

In contrast to the HSE06 potential, the PBE-D2 functional is not sufficient to calculate reliable refractive indices. For the following investigation, the primitive cell of UiO-66 was fully relaxed using the PBE-D2 functional with a plane-wave kinetic energy cutoff set to 1000 eV and *Γ*-point sampling.[4,5]

The PBE XC functional is known for underestimating the band gap. Therefore, the band gap of UiO-66 resulting when using the PBE-D2 XC functional in the band structure calculation is much too small: 3.056 eV (see Fig. S27) versus a simulated value of 4.25 eV (HSE06 functional-based) and an experimental one of 4.05 eV. In the further calculations, the maximum of the absorption coefficient and the refractive index both show a large red shift. UiO-66 is transparent in the visible region, but the PBE-D2 electronic structure calculation results suggest that it shows absorption of blue light. This underestimation of the band gap and the resulting red shift of the RI dispersion curve leads to a plateau of the RI dispersion in the blue region of the visible range of light, causing a large dispersion of the RI in the visible region (see Fig. S28). Also, over the whole range of visible light, the refractive index values calculated based on the PBE XC functional are considerably higher than those based on the HSE06 functional (Fig. S28). The PBE-based results would suggest that UiO-66 is a highly refractive material which is not the case.

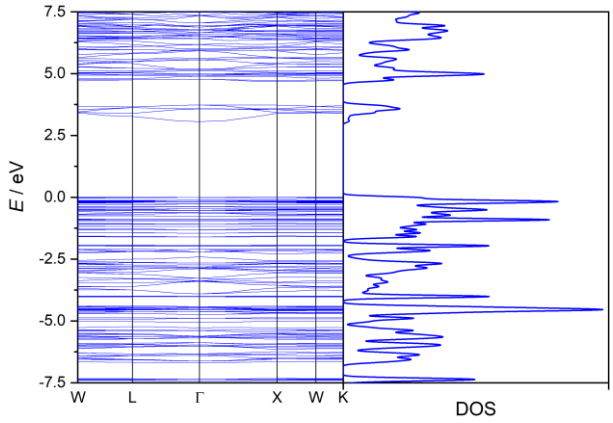

Figure S28. UiO-66 band structure with DOS calculated with the PBE-D2 functional. The band gap determined from this band structure is 3.056 eV.

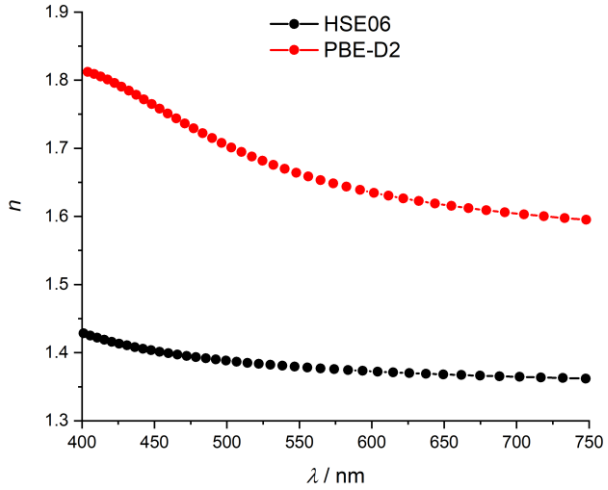

Figure S27. Comparison of the refractive index dispersion of UiO-66 calculated with HSE06 and PBE-D2, respectively.

References

[1] C. Heldmann, M. Schulze, G. Wegner, *Macromolecules* **1996**, *29*, 4686.
[2] H. Hahm, K. Yoo, H. Ha, M. Kim, *Inorg. Chem.* **2016**, *55*, 7576.
[3] G. C. Shearer, S. Chavan, J. Ethiraj, J. G. Vitillo, S. Svelle, U. Olsbye, C. Lamberti, S. Bordiga, K. P. Lillerud, *Chem. Mater.* **2014**, *26*, 4068.
[4] J. P. Perdew, K. Burke, M. Ernzerhof, *Phys. Rev. Lett.* **1996**, *77*, 3865.
[5] S. Grimme, *J. Comput. Chem.* **2006**, *27*, 1787.